

# Nicotinamide-Appended Fluorophores as Fluorescent Redox Sensors

Kathryn G. Leslie,<sup>A</sup> Jacek L. Kolanowski,<sup>A</sup> Natalie Trinh,<sup>A</sup>  
Serena Carrara,<sup>B</sup> Matthew D. Anscomb,<sup>A</sup> Kylie Yang,<sup>A</sup> Conor F. Hogan,<sup>B</sup>  
Katrina A. Jolliffe,<sup>A,C</sup> and Elizabeth J. New<sup>A,C</sup>

<sup>A</sup>University of Sydney, School of Chemistry, Sydney, NSW 2006, Australia.

<sup>B</sup>Department of Chemistry and Physics, La Trobe Institute for Molecular Science, La Trobe University, Melbourne, Vic. 3086, Australia.

<sup>C</sup>Corresponding authors. Email: [kate.jolliffe@sydney.edu.au](mailto:kate.jolliffe@sydney.edu.au); [elizabeth.new@sydney.edu.au](mailto:elizabeth.new@sydney.edu.au)

Fluorescent sensors have proved invaluable in elucidating the regulation and dysregulation of redox processes in biology, but understanding of the breadth of biological redox reactions requires development of new sensors based on a range of sensing groups with varied reduction potentials. The aim of this work was to investigate the use of nicotinamide as a redox switch when conjugated to two classes of amino-fluorophores. We prepared four fluorophore conjugates based on 7-aminocoumarins and 4-amino-1,8-naphthalimides via the nicotinamide Zincke salt. These conjugates all showed clear fluorescence changes in response to chemical reduction, but this reduction was irreversible both chemically and electrochemically. The reduction behaviour of the 1,8-naphthalimides was investigated further by spectroelectrochemistry, revealing that conjugate **NNpR1** showed the clearest spectral changes on both chemical and electrochemical reduction. Cells dosed with **NNpR1** and maintained under hypoxic conditions exhibited a significantly higher green : blue fluorescence ratio than cells cultivated under normoxia, confirming the potential of this molecule as a sensor for reductive biological environments.

Manuscript received: 15 August 2019.

Manuscript accepted: 6 September 2019.

Published online: 15 October 2019.

## Introduction

Redox reactions underpin a multitude of biological processes, from the Fe<sup>II</sup>/Fe<sup>III</sup> redox couple essential for carrying oxygen in haemoglobin to the electron transport chain central to aerobic respiration. The reversibility of redox processes is critical to cellular signalling and function, and there is therefore a need to reversibly sense redox changes in biology, rather than just to measure end-point redox status. This can be achieved by fluorescence imaging using reversible fluorescent sensors.<sup>[1]</sup> Such sensors should have measurable fluorescence changes (emission intensity, wavelength or lifetime) on oxidation and reduction, and a biologically relevant reduction potential. In order to access different biological events, it is important that new sensors are developed based on different redox switches.

One effective method for design of redox sensors is to identify redox switches that already play a role in biological systems.<sup>[2]</sup> For example, fluorescent redox sensors have been reported based on the cysteine–disulfide transformation,<sup>[3,4]</sup> while we and others have demonstrated the utility of the vitamin flavin, ubiquitous in biological systems in the form of the redox cofactor flavin adenine dinucleotide (FAD), as a redox switch.<sup>[5,6]</sup> The other predominant redox cofactor is nicotinamide adenine dinucleotide (NAD<sup>+</sup>), and its analogue nicotinamide adenine dinucleotide phosphate (NADP<sup>+</sup>), and we therefore became interested in investigating the potential of

nicotinamide as a redox switch. Like flavins, nicotinamides are reversibly oxidised and reduced (Fig. S1, Supplementary Material), but with markedly different reduction potentials (−316 mV versus standard hydrogen electrode (SHE) for NAD<sup>+</sup>; −219 mV versus SHE for FAD).

There has been one previous report of a fluorophore–nicotinamide conjugate, **Perylene–NAD**, in which nicotinamide was linked to perylene.<sup>[7]</sup> The fluorescence of perylene was quenched by reduced nicotinamide via photoinduced electron transfer, and this quenching was alleviated on oxidation of the nicotinamide. The reversibility of this system was demonstrated in organic solvent with the sequential addition of the reductant sodium cyanoborohydride and oxidant tetrachloro-1,4-benzoquinone (TCBQ). More recently, we have reported **GdNR1**, a reversible, redox-responsive magnetic resonance imaging (MRI) contrast agent.<sup>[8]</sup> **GdNR1** is a Gd complex with a nicotinamide-conjugated DO3A ligand that undergoes a 2.5-fold increase in relaxivity on reduction. Encouraged by the aqueous reversibility of oxidation and reduction that we had observed, and the differential effects of oxidised and reduced nicotinamide on fluorophore emission reported by Yan et al.,<sup>[7]</sup> we sought to develop new fluorophore–nicotinamide conjugates to identify the best scaffold for a biological redox sensor. We report here our work in developing conjugates of nicotinamide with coumarins and 4-amino-1,8-naphthalimides.

## Results and Discussion

### Sensor Design and Synthesis

We chose fluorophores based on 7-aminocoumarin and 4-amino-1,8-naphthalimide as they bear an amine group essential for the intramolecular charge transfer (ICT) involved in the fluorescence mechanism of both classes of fluorophore. We reasoned that extending the conjugation with a nicotinamide would suppress ICT from the amine lone pair, with fluorescence restored on reduction. Based on coumarin 120 and coumarin 151 respectively, we proposed nicotinamide coumarin redox sensors 1 and 2 (**NCR1** and **2**; Fig. 1), and we proposed nicotinamide naphthalimide redox sensor 1 (**NNpR1**) based on the commonly employed *N*-butyl-4-amino-1,8-naphthalimide. In keeping with our interest in disubstitution of naphthalimides,<sup>[9]</sup> we also designed analogue **NNpR2**, in which we inserted the nicotinamide group at the C6 position on the ring.

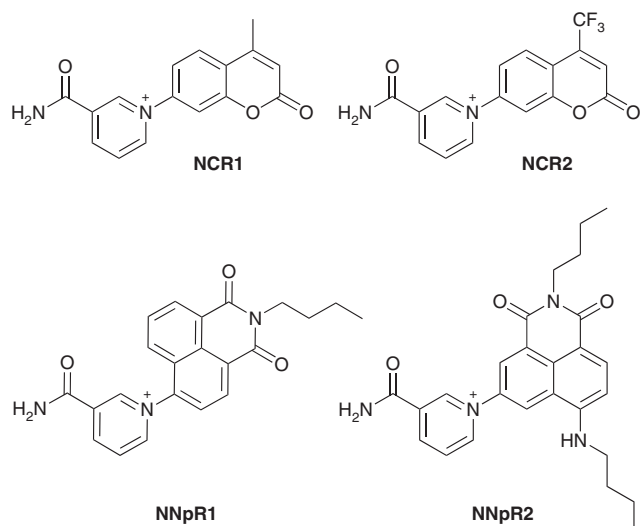
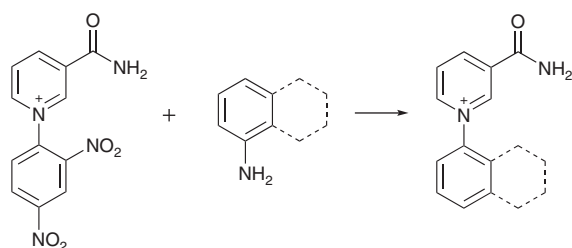


Fig. 1. Nicotinamide-fluorophore conjugates prepared in the present work.



Scheme 1. Synthesis of generic nicotinamide-fluorophore conjugate from the nicotinamide Zincke salt.

Free  $\text{NAD}^+$  is estimated to be 700 times more abundant than NADH in the cytoplasm of mammalian cells,<sup>[10]</sup> and  $\sim 3$ – $10$  times more abundant across all cellular compartments.<sup>[11]</sup> We therefore hypothesised that these proposed nicotinamide-fluorophore conjugates would remain in the oxidised form in healthy cellular environments, and would be poorly sensitive to oxidative stress. However, we anticipated that they might be suitable to report an increase in the reductive capacity of the cell, making them potential probes for hypoxic conditions.

It has previously been shown that nicotinamides can be readily conjugated to anilines or amines using the Zincke reaction,<sup>[12,13]</sup> and this approach was employed in the synthesis of the target compounds. The required derivatised fluorophores were commercially available, or were prepared by previously reported methods,<sup>[9]</sup> and were reacted with the Zincke salt of nicotinamide to give the **NCR** and **NNpR** analogues (Scheme 1).

### Fluorescence Studies

Preliminary photophysical characterisation of the four compounds showed that although the naphthalimide-based compounds showed similar excitation and emission profiles to the parent amino-fluorophores, the coumarin excitation and emission peaks were somewhat shifted (Table 1). As expected, the fluorescence of the naphthalimides was considerably red-shifted with respect to that of the coumarins, with excitation wavelengths being far better suited to confocal microscopy set-ups.

The fluorescence responses of the compounds to reduction and subsequent oxidation were investigated by chemical titration with reducing agent sodium dithionite and oxidising agent hydrogen peroxide. Large spectral changes were observed for all four probes on reduction with dithionite (Fig. 2), but this could not be reversed on subsequent addition of hydrogen peroxide (Fig. S2, Supplementary Material). **NNpR1** and **NNpR2** showed fluorescence increases on reduction consistent with restoration of the ICT process as the nicotinamide group was reduced, whereas **NCR1** and **NCR2** displayed modest decreases in fluorescence on reduction, indicating that this ICT-based process does not predominate for these coumarins. **NNpR1** and **NNpR2** both displayed some level of ratiometricity in their fluorescence response to reduction, rather than simply a change in emission intensity. This is a favourable property for fluorescent probes as a change in the ratio of emission, as opposed to an increase in intensity, gives an internal calibration that eliminates the effect of probe concentration in analysis, and reports only on analyte presence.<sup>[17]</sup>

### Electrochemical Studies

The redox responses of the probes were further investigated using cyclic voltammetry. Each compound exhibited multiple irreversible redox processes, typically one oxidation and multiple reductions, though the response for **NCR1** suggests a

Table 1. Excitation and emission maxima in ethanol for parent amino-fluorophore and nicotinamide-fluorophore conjugate

	Parent amino-fluorophore		Nicotinamide-fluorophore conjugate	
	$\lambda_{\text{ex}}$ [nm]	$\lambda_{\text{em}}$ [nm]	$\lambda_{\text{ex}}$ [nm]	$\lambda_{\text{em}}$ [nm]
<b>NCR1</b>	353 <sup>[14]</sup>	451 <sup>[14]</sup>	324	484
<b>NCR2</b>	383 <sup>[15]</sup>	485 <sup>[15]</sup>	326, 372	463
<b>NNpR1</b>	437 <sup>[16]</sup>	532 <sup>[16]</sup>	424	518
<b>NNpR2</b>	469 <sup>[9]</sup>	546 <sup>[9]</sup>	458	548

second oxidation process at higher potentials. This is consistent with the chemical irreversibility observed in the dithionite titrations, and indicates that these probes would be unsuitable for reporting fluctuations in a reducing environment, but could report on the least reducing environment experienced.

Given the broadly similar electrochemical results for all molecules, we decided to focus on the naphthalimide systems because of their more suitable fluorescence properties, and to study these systems further using fluorescence spectroelectrochemistry.

Spectroelectrochemistry experiments were performed by biasing a platinum gauze working electrode at a suitably negative potential while monitoring changes in the absorption spectrum. The potentials were chosen based on the reduction potentials observed in the cyclic voltametric responses shown in Fig. 3. Electrolysis at the first (i.e. the least negative) reduction potential for both **NNpR1** and **NNpR2** ( $-0.53$  and  $-0.64$  V versus saturated calomel electrode (SCE) respectively) did not result in significant changes in the absorption spectrum of the compound (Fig. S3a, c, Supplementary Material). However, reduction at the second peak for **NNpR1** ( $-1.05$  V versus SCE) induced marked changes in the visible region, with absorption bands between 400 and 600 nm increasing in intensity with electrolysis time (Fig. S3b, Supplementary Material). A similar pattern was observed at the third reduction potential of  $-1.68$  V versus SCE (Fig. 4a) though these peaks grew more rapidly due to the higher overpotential. For **NNpR2**, reduction at the second or third reduction peak ( $-1.40$  and  $-1.8$  V versus SCE) induced multiple changes in the spectrum (Fig. S3d, Supplementary Material and Fig. 4b). These changes evolved without an isosbestic points, indicating the existence of several species in solution and pointing to a complex, multistep reduction process.

The effect of electrochemical reduction on the fluorescence emission spectra of the two compounds was investigated in a similar way by biasing the electrode at  $-1.68$  and  $-1.80$  V

versus SCE for **NNpR1** and **NNpR2** respectively, with excitation at 350 nm. For **NNpR1**, a decrease in the emission at 480 nm was observed, followed by the emergence of a new emission band at 510 nm (Fig. 5a). This change in fluorescence was visually evident under UV light when comparing the solution of **NNpR1** before reduction (Fig. S4a, Supplementary Material) with the solution that underwent extensive electrolysis (Fig. S4b, Supplementary Material). Similar changes in fluorescence emission were observed for **NNpR2** (Fig. S4c–d, Supplementary Material). Before reduction, the solution appeared orange-emissive and highly turbid as the compound is poorly soluble in acetonitrile. This is reflected in the emission profile, which is broad and featureless, peaking at 560 nm and showing a long tail up to 800 nm. On reduction, there was an initial decrease in the emission at 560 nm, followed by a subsequent increase of emission at both 560 and 630 nm. Though the fluorescence spectroelectrochemical response is complicated somewhat by the increased solubility of the reduced product or products, it is clear that electrochemical reduction of **NNpR2** results in a distinct change in fluorescence colour.

As **NNpR1** showed the clearest ratiometric changes on chemical and electrochemical reduction, and it was soluble and stable to reduction, we chose this as the most promising candidate for evaluation in cellular studies.

#### Confocal Microscopy Studies

Given the clear spectral changes observed on chemical and electrochemical reduction of **NNpR1**, it was taken forward into studies in monolayer A549 human lung carcinoma cells. **NNpR1** was not found to be toxic up to a concentration of 100  $\mu\text{M}$  for a 4-h incubation (Fig. S5, Supplementary Material). A549 cells were therefore incubated with **NNpR1** for 30 min to determine whether the oxidised or reduced form would be observed under normoxic conditions. After 30-min excitation,

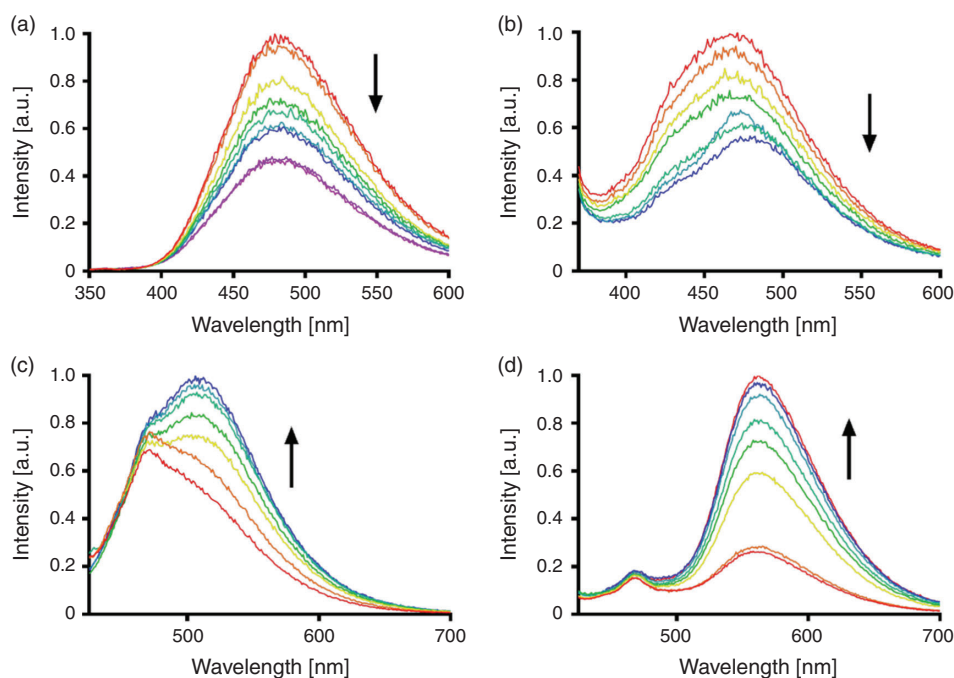


**Fig. 2.** Normalised fluorescence emission spectra of (a) **NCR1** (10  $\mu\text{M}$ ,  $\lambda_{\text{ex}}$  320 nm); (b) **NCR2** (10  $\mu\text{M}$ ,  $\lambda_{\text{ex}}$  350 nm); (c) **NNpR1** (10  $\mu\text{M}$ ,  $\lambda_{\text{ex}}$  405 nm); (d) **NNpR2** (10  $\mu\text{M}$ ,  $\lambda_{\text{ex}}$  405 nm) in 20 : 80 MeCN/HEPES buffer (5 mM), on addition of sodium dithionite (10 to 100  $\mu\text{M}$ ). Arrows indicate increasing sodium dithionite concentration.

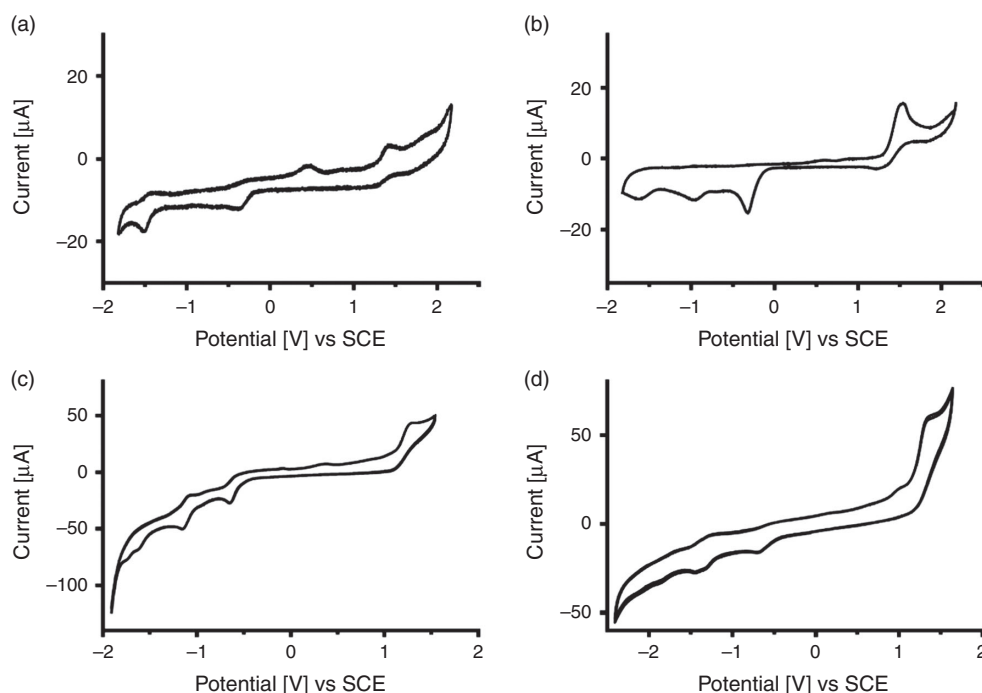


**Fig. 3.** Cyclic voltammograms of (a) **NCR1**; (b) **NCR2**; (c) **NNpR1**; and (d) **NNpR2** (1 mM, with 0.1 M tetrabutylammonium hexafluorophosphate in MeCN,  $100 \text{ mV s}^{-1}$ ).

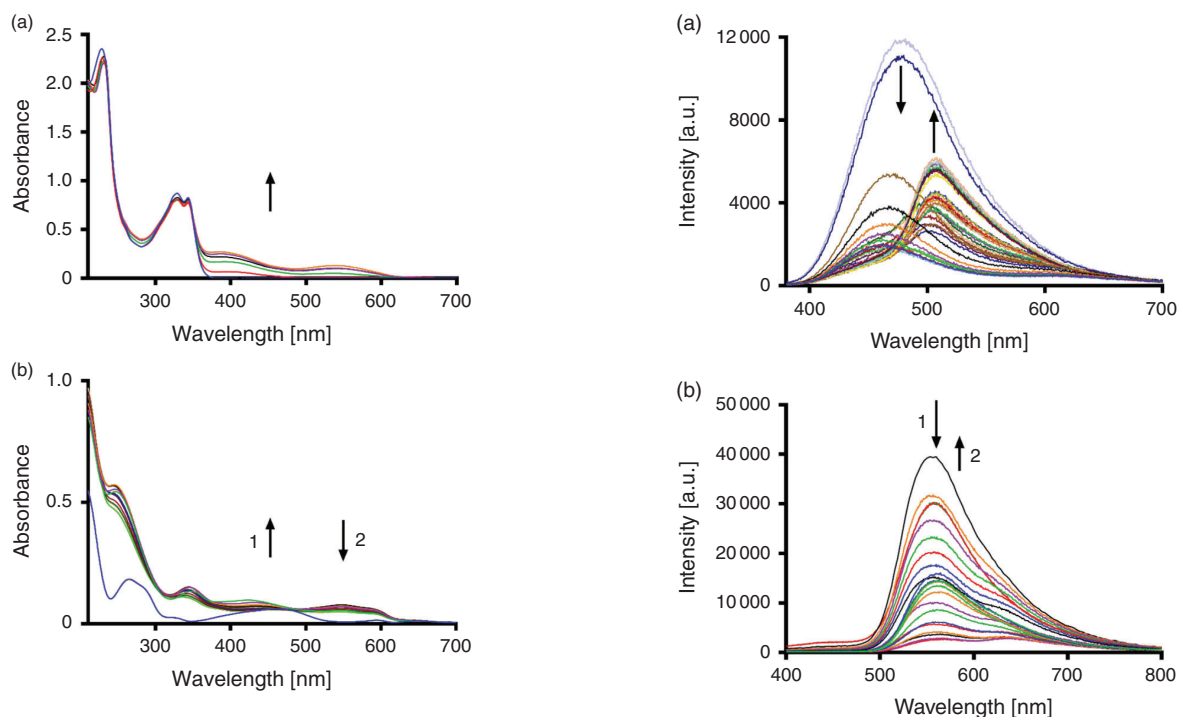


**Fig. 4.** UV-visible absorption spectra of (a) **NNpR1** on reduction at  $-1.68 \text{ V}$ , and (b) **NNpR2** on reduction at  $-1.80 \text{ V}$  (1 mM, with 0.1 M tetrabutylammonium hexafluorophosphate in MeCN).

intracellular fluorescence could be observed (Fig. 6a), and the spectrum of the compound in cells matched the spectrum of the reduced compound in fluorimetry studies, with strong green emission at 520 nm (Fig. 6b). This is an interesting result, because the reduction potential of **NNpR1** is lower than that of hypoxia probes that we have previously reported to be reduced far more slowly in normoxic cells,<sup>[18]</sup> and likely indicates that

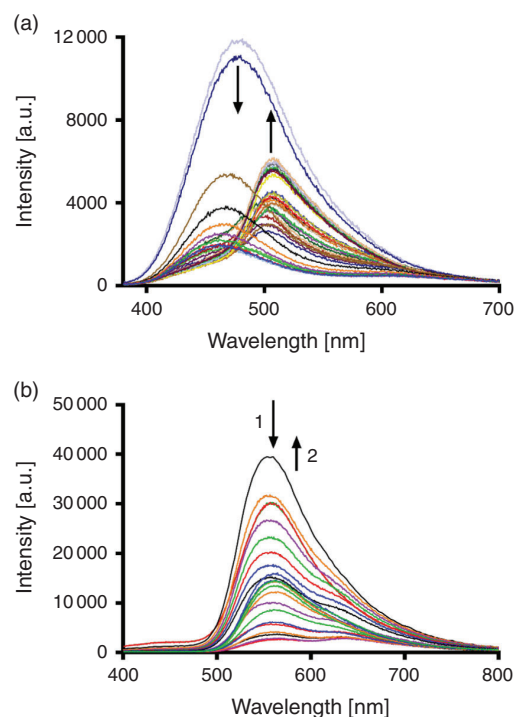


**Fig. 5.** (a) Fluorescence spectra of **NNpR1** on reduction at  $-1.68 \text{ V}$  versus SCE. Arrows indicate spectral changes accompanying reduction. (b) Fluorescence spectra of **NNpR2** on reduction at  $-1.80 \text{ V}$  versus SCE (1 mM, with 0.1 M tetrabutylammonium hexafluorophosphate in MeCN,  $\lambda_{\text{ex}} 350 \text{ nm}$ ). Arrows indicate decrease (1) and subsequent increase (2) of emission intensity upon reduction.

there is enzymatic reduction of the nicotinamide moiety, perhaps by one of the many oxidoreductases that are biologically coupled to reduction of  $\text{NAD}^+$ .

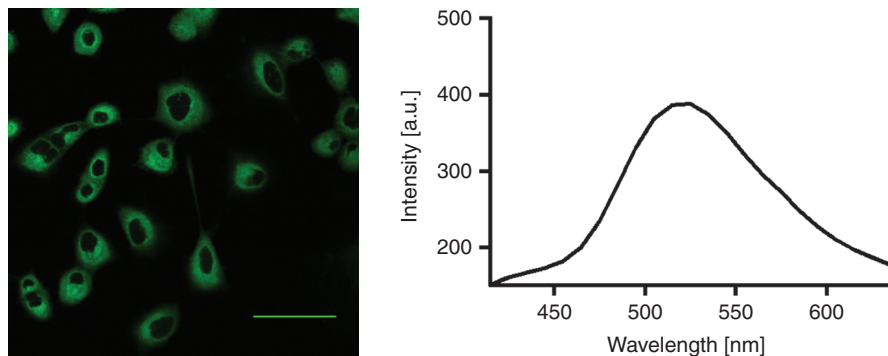


**Fig. 6.** Confocal microscope images of A549 cells incubated with **NNpR1** (100  $\mu$ M, 30 min), with 405-nm excitation. (a) Fluorescence emission, and (b) spectral scan. Scale bar represents 50  $\mu$ m.

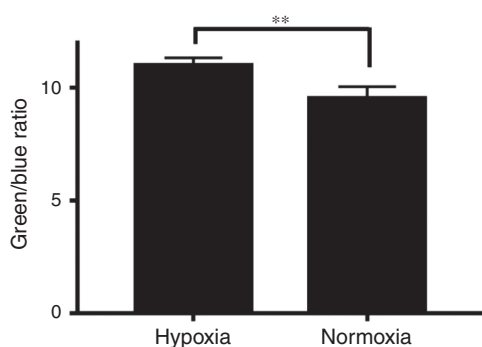
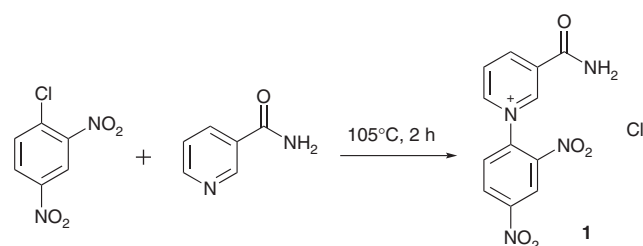


**Fig. 7.** Average intensity ratio between the green (490–590 nm) and blue (440–490 nm) emission of **NNpR1** in A549 cells under hypoxic (1% oxygen) or normoxic (19% oxygen) conditions after 3 h. Error bars represent the standard deviation ( $n = 3$ );  $**P = 0.0016$ .

As **NNpR1** gives a ratiometric response to reduction, we then sought to investigate whether it would be possible to observe differences between normoxic and hypoxic conditions, as small differences in the rate of turn-on that would be unreliable to measure merely on an intensity basis are potentially detectable when measuring a ratio between the blue and green portions of the emission spectrum. A549 cells were dosed with **NNpR1** (200  $\mu$ M) for 30 min, washed, and then incubated for 3 h either under hypoxia (1% oxygen) or normoxia (19% oxygen). The cells were then imaged with fluorescence emission in two channels, blue (440–490 nm) and green (490–590 nm). Although a similar green:blue ratio was observed in hypoxic and normoxic cells, the ratio was clearly higher in the hypoxic cells, suggesting **NNpR1** is reduced at a faster rate under hypoxia (Fig. 7). The high green:blue ratio observed is consistent with **NNpR1** being more predominantly in the reduced form in both hypoxic and normoxic cells; therefore, to improve the ratiometric sensing ability of this probe, it is also necessary to improve its selectivity towards hypoxia and minimise reduction of the probe by normoxic cells. This requires tuning the sensing group, possibly by decreasing its reduction potential.

## Conclusions

This work has demonstrated how altering the electronic properties of a sensing group can lead to marked changes in the emission profiles of amino-fluorophores. Reduction of nicotinamide conjugated to 7-aminocoumarin or 4-amino-1,8-naphthalimide scaffolds led to changes in fluorescence



**Scheme 2.** Synthesis of 3-carbamoyl-1-(2,4-dinitrophenyl)pyridine-1-ium (**1**).

emission, but this process was not reversible either chemically or electrochemically. For the development of reversible sensors based on naphthalimides, conjugation to aliphatic rather than aromatic groups will be required.

Spectroelectrochemical studies helped to identify **NNpR1** as the most promising candidate for further studies, and this probe was able to discriminate cells in hypoxic from those in normoxic conditions by measuring the change in ratio of emission intensity in the green and blue channels.

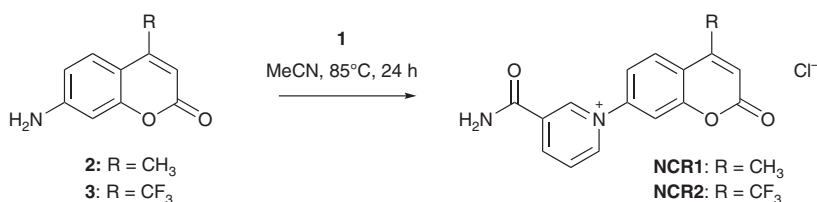
## Experimental

### Synthetic Procedures

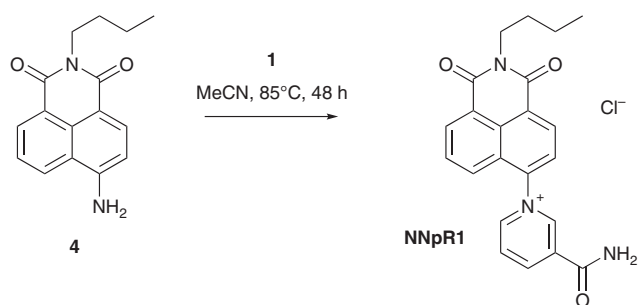
7-Amino-4-methylcoumarin (**2**) and 7-amino-4-trifluoromethylcoumarin (**3**) were purchased from Sigma-Aldrich. Naphthalimides **4** and **5** were synthesised as previously reported.<sup>[9]</sup>

### Synthesis of 3-Carbamoyl-1-(2,4-dinitrophenyl)pyridine-1-ium (**1**, Scheme 2)

Nicotinamide (0.6 g, 5 mmol) and chloro-2,4-dinitrobenzene (1.11 g, 5.5 mmol) were heated together at 105°C and stirred for 2 h. The reaction was cooled to room temperature, then the mixture was dissolved in methanol (2 mL), and precipitated with ether (4  $\times$  10 mL). The precipitate was filtered each time and combined precipitates were dried to give 3-carbamoyl-1-(2,4-dinitrophenyl)pyridine-1-ium as a sticky amber solid (1.42 g, 88%).  $\delta_{\text{H}}$  (400 MHz, [D6]DMSO) 9.90 (s, 1H), 9.52 (dt,  $J$  6.3, 1.4, 1H), 9.33 (dt,  $J$  8.3, 1.4, 1H), 9.12 (d,  $J$  2.5, 1H), 8.98 (dd,  $J$  8.6, 2.5, 1H), 8.89 (s, 1H), 8.54 (dd,  $J$  8.2, 6.3, 1H), 8.46 (d,  $J$  8.8, 1H), 8.28 (s, 1H).  $\delta_{\text{C}}$  (125 MHz, [D6]DMSO) 162.9, 149.7, 148.0, 147.1, 146.8, 143.4, 139.0, 134.1, 132.3, 130.7, 128.2, 121.9.



**Scheme 3** Synthesis of nicotinamide–coumarins **NCR1** and **NCR2**.



**Scheme 4.** Synthesis of nicotinamide–naphthalimide **NNpR1**.

#### General Procedure for Nicotinamide–Coumarin Synthesis (**NCR1–2**, *Scheme 3*)

A solution containing the corresponding coumarin (**2** or **3**, 1 equiv.) and **1** (1 equiv.) was heated under reflux conditions in acetonitrile over 24 h and then left to cool. The resulting precipitate was filtered and washed with cold acetonitrile, and recrystallised from methanol to give the product as described below.

**NCR1**: beige solid (69%).  $\delta_{\text{H}}$  (500 MHz,  $\text{D}_2\text{O}$ ) 9.63 (m, 1H), 9.40 (dt,  $J$  6.2, 1.2, 1H), 9.17 (dt,  $J$  8.2, 1.4, 1H), 9.45 (m, 1H), 8.19 (d,  $J$  8.6, 1H), 7.9 (d,  $J$  2.3, 1H), 7.85 (dd,  $J$  8.6, 2.3, 1H), 6.62 (d,  $J$  1.2, 1H), 2.62 (d,  $J$  2.6, 3H).  $\delta_{\text{C}}$  (125 MHz,  $\text{D}_2\text{O}$ ) 154.7, 153.1, 146.6, 145.6, 144.5, 143.9, 134.1, 128.6, 127.9, 122.7, 120.4, 116.0, 113.3, 18.0.  $m/z$  (high-resolution mass spectrometry (HRMS) positive electrospray ionisation (+ESI)) 281.0920; calc. for  $\text{C}_{16}\text{H}_{13}\text{N}_2\text{O}_3^+$  281.0921  $[\text{M}]^+$ .

**NCR2**: beige solid (55%).  $\delta_{\text{H}}$  (500 MHz,  $\text{D}_2\text{O}$ ) 9.71 (m, 1H), 9.42 (dt,  $J$  6.2, 1.3, 1H), 9.19 (dt,  $J$  8.2, 1.4, 1H), 8.47 (m, 1H), 8.25 (dd,  $J$  8.8, 1.5, 1H), 8.06 (d,  $J$  2.3, 1H), 7.92 (dd,  $J$  8.7, 2.4, 1H), 7.25 (s, 1H).  $\delta_{\text{C}}$  (125 MHz,  $\text{D}_2\text{O}$ ) 165.5, 160.8, 154.3, 146.8, 146.1, 144.7, 140.2 (q,  $J_{\text{C-F}}$  33.5), 134.3, 128.8, 128.1, 122.4, 121.1, 120.2, 119.0, 116.6, 114.2.  $m/z$  (HRMS +ESI) 335.0637; calc. for  $\text{C}_{16}\text{H}_{10}\text{F}_3\text{N}_2\text{O}_3^+$  335.0638  $[\text{M}]^+$ .

#### General Procedure for Nicotinamide–Naphthalimide Synthesis (**NNpR1–2**)

A solution containing the corresponding naphthalimide (**4** or **5**; 1.1 equiv.) and **1** (1 equiv.) was heated under reflux conditions in acetonitrile over 48 h and then left to cool. The resulting precipitate was filtered and washed with cold acetonitrile to give the product as described below.

**NNpR1** (*Scheme 4*): grey solid (75%).  $\delta_{\text{H}}$  (400 MHz, [D6] DMSO) 9.92 (s, 1H), 9.55 (d,  $J$  6.1, 1H), 9.37 (d,  $J$  8.0, 1H), 8.92 (s, 1H), 8.76 (d,  $J$  7.6, 1H), 8.67 (d,  $J$  6.9, 1H), 8.59–8.53 (m, 1H), 8.40 (d,  $J$  8.0, 1H), 8.25 (s, 1H), 8.06–7.97 (m, 2H), 4.10 (t,  $J$  7.4, 2H), 1.71–1.62 (m, 2H), 1.43–1.32 (m, 2H), 0.98–0.92 (t,  $J$  7.5, 3H).  $\delta_{\text{C}}$  (125 MHz, [D6] DMSO) 163.5, 162.9, 162.8, 148.4, 146.8, 146.7, 143.1, 134.7, 132.4, 130.8, 130.1, 128.9,

128.7, 128.4, 126.8, 126.4, 125.4, 123.0, 30.0, 20.3, 14.2.  $m/z$  (ESIMS)  $[\text{M}]^+$  374; (HRMS +ESI) 374.1498; calc. for  $\text{C}_{22}\text{H}_{20}\text{N}_3\text{O}_3^+$  374.1499  $[\text{M}]^+$ .

**NNpR2** (*Scheme 5*): orange solid (68%).  $\delta_{\text{H}}$  (500 MHz, [D6] DMSO) 9.92 (s, 1H), 9.67 (d,  $J$  6.0, 1H), 9.54 (s, 1H), 9.15 (d,  $J$  8.4, 1H), 8.94–8.89 (m, 2H), 8.50–8.46 (dd,  $J$  7.8, 6.5, 1H), 8.40 (d,  $J$  8.6, 1H), 8.30–8.26 (m, 2H), 6.94 (d,  $J$  8.65, 1H), 4.06 (t,  $J$  7.6, 2H), 3.47–3.40 (m, 2H), 1.77–1.69 (m, 2H), 1.66–1.58 (m, 2H), 1.49–1.41 (m, 2H), 1.40–1.30 (m, 2H), 0.98–0.90 (m, 6H).  $\delta_{\text{C}}$  (125 MHz, [D6] DMSO) 163.3, 163.1, 163.0, 152.0, 147.4, 145.6, 145.1, 139.0, 136.7, 134.4, 130.4, 128.6, 126.8, 126.3, 124.0, 120.7, 107.6, 105.7, 43.2, 30.4, 30.2, 20.3, 20.2, 14.2.  $m/z$  (ESIMS)  $[\text{M}]^+$  445; (HRMS +ESI) 445.2234; calc. for  $\text{C}_{26}\text{H}_{29}\text{N}_4\text{O}_3^+$  445.2234  $[\text{M}]^+$ .

#### Fluorescence Spectroscopy

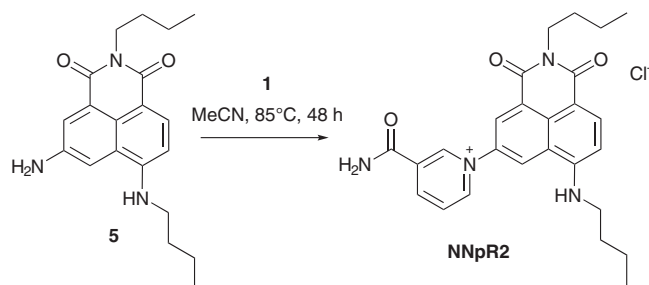
All fluorescence spectra were recorded on a Varian Cary Eclipse fluorometer in 1 cm pathlength quartz cuvettes. The emission spectra of 10  $\mu\text{M}$  solutions in 20:80 MeCN/HEPES (HEPES = 4-(2-hydroxyethyl)-1-piperazineethanesulfonic acid) buffer (5 mM) were recorded with 10  $\mu\text{L}$  aliquots of freshly prepared 1 M sodium dithionite in phosphate-buffered saline (PBS) buffer until no further change in fluorescence was observed.

#### Cyclic Voltammetry

Electrochemical measurements were performed using a BAS 100B/W electrochemical analyser. A single-compartment cell was used, consisting of a glassy carbon working electrode, a platinum wire auxiliary electrode, and an electrolysed Ag/AgCl wire reference electrode. Cyclic voltammograms (CVs) were collected using a 1 mM solution of the analyte in MeCN, with 0.1 M tetrabutylammonium hexafluorophosphate as a supporting electrolyte. Prior to each experiment, the solution was purged with Ar. Uncompensated resistance between the working and the reference electrodes was corrected by using  $iR$  compensation. Measurements were converted to a standard hydrogen electrode reference (versus SHE) for comparison with the literature.

#### Spectroelectrochemistry

The electrochemical characterisation of the molecules was carried out in acetonitrile with 0.2 M tetrabutylammonium hexafluorophosphate (TBAPF<sub>6</sub>). Oxygen was removed by purging the MeCN solution with high-purity argon. A typical three-electrode cell was employed, which was composed of a glassy carbon (GC) working electrode (3-mm diameter, CH Instruments, Austin, TX, USA), a platinum wire as counter, and a silver wire as quasi-reference (QRE) electrode. A CHI620 electrochemical workstation (CH Instruments) was employed to record the CVs. The potential of the reference electrode was



**Scheme 5.** Synthesis of nicotinamide–naphthalimide **NNpR2**.

calibrated after each measurement using ferrocene/ferrocenium ( $\text{Fc}/\text{Fc}^+$ ) redox couple as the internal standard. The formal potential of  $\text{Fc}/\text{Fc}^+$  is 0.464 V in MeCN against the KCl SCE. The GC electrodes before experiments were polished with a 0.3  $\mu\text{m}$  alumina suspension rinsed with deionised water and ethanol. The standard potentials were calculated as the average value between cathodic and anodic peak potentials, when the processes were reversible or quasi-reversible. All CVs were carried out at scan rate 0.1  $\text{V s}^{-1}$ .

UV/vis-SEC (SEC = spectroelectrochemistry) and fluorescence-SEC experiments were carried out using a Pt gauze as working electrode, a Pt wire as counter, and a silver wire as quasi-reference electrode. UV-visible spectra were collected using a Cary Series UV-visible spectrophotometer (Agilent) with a 1 mm path length quartz cuvette, a spectral bandwidth of 1 nm, a signal averaging time of 0.1 s, a data interval of 0.25 nm, and a scan rate of 150  $\text{nm min}^{-1}$ . Steady-state emission spectra were collected on a Nanolog spectrofluorometer (Horiba Jobin Yvon IBH). A 450-W xenon arc lamp was used to excite the complexes using a 1200  $\text{g mm}^{-1}$  grating blazed at 330 nm excitation monochromators, a 1200  $\text{g mm}^{-1}$  grating blazed at a 500 nm emission monochromator, and a thermoelectrically cooled TBX picosecond single-photon detector. Emission spectra were corrected for source intensity, gratings, and detector response.

### Cell Experiments

#### Cell Line

All cellular studies used the adenocarcinoma human alveolar basal epithelial cell line A549. Cells were maintained in exponential growth as monolayers in Advanced Dulbecco's Modified Eagles Medium (ADMEM) supplemented with 1.25 % glutamine (G) and 2 % foetal bovine serum (FBS). Cells were incubated at 37°C in 5 % v/v  $\text{CO}_2$  under humidified conditions. These cell lines were subcultured using 0.25 % trypsin to facilitate dislodgement of cells from the flask.

#### Cytotoxicity

A549 cells were plated into a 96-well plate and grown until ~80 % confluent. Cells were incubated with **NNpR1** (100  $\mu\text{M}$ , four replicates) for 3.5 h alongside control cells. Alamar Blue was then added and cells incubated for a further 3 h. Fluorescence output was read at 590 nm ( $\lambda_{\text{ex}}$  570 nm) on a PerkinElmer EnSpire multimedia plate reader, and the averaged value for repeats reported as a percentage of the control.

#### Imaging in Normoxia (Control Experiment)

A total of  $1 \times 10^5$  A549 cells were seeded in a poly-D-lysine coated MatTek dish and allowed to adhere for 36 h. Afterwards,

probe solutions in media were prepared by first dissolving the probe in DMSO, then quickly adding it to the media. The cells were then incubated in the probe solution for 30 min. Afterwards, the cells were washed with PBS and put in FluoroBrite™ media. They were imaged in an Olympus FV3000 microscope using a 60 $\times$  water objective and 405-nm laser excitation. Spectral scans were recorded by measuring the fluorescence emission in 10-nm bands every 10 nm.

#### Hypoxic Imaging Experiment

A549 cells were seeded at  $1 \times 10^5$  cells per MatTek dish and allowed to adhere overnight. The medium was removed, and the cells were dosed with probe (200  $\mu\text{M}$ , 30 min), rinsed thrice with PBS, then 0.5 mL FluoroBrite™ media supplemented with 1 % glutamine, and 2 % FBS was added. One dish was placed under normoxia (19 % oxygen, 5 %  $\text{CO}_2$ ) in a humidified incubator. The other dish was placed into an Okolab hypoxic stage-top incubator for 1 h, then cycled between 15 min at 1 % oxygen and 15 min at 19 % oxygen (three cycles). After the incubation had finished, both dishes were imaged using a spectral scanner (415–615 nm, 10-nm band width, 10-nm step size) and 403.6-nm laser excitation.

### Supplementary Material

Supplementary figures are available on the Journal's website.

### Conflicts of Interest

The authors declare no conflicts of interest.

### Acknowledgements

The authors would like to acknowledge the Australian Research Council (grant numbers DP150100649, DP180101353, DP180101897) for funding, the Westpac Scholars Trust for a Research Fellowship (EJN), the University of Sydney for a SOAR Fellowship (EJN), and the Australian government for Research Training Program Scholarships (KGL, NT, KY). They also acknowledge the scientific and technical assistance of the Australian Microscopy and Microanalysis Research Facility at the Australian Centre for Microscopy and Microanalysis (ACMM), and thank Cecile Elgindy and Phillip Karpati for assistance with initial synthetic studies.

### References

- [1] A. Kaur, J. L. Kolanowski, E. J. New, *Angew. Chem. Int. Ed.* **2016**, *55*, 1602. doi:10.1002/ANIE.201506353
- [2] A. Kaur, E. J. New, *Acc. Chem. Res.* **2019**, *52*, 623. doi:10.1021/ACS.ACCOUNTS.8B00368
- [3] K. Lee, V. Dzubeck, L. Latshaw, J. P. Schneider, *J. Am. Chem. Soc.* **2004**, *126*, 13616. doi:10.1021/JA047300R
- [4] E. W. Miller, S. X. Bian, C. J. Chang, *J. Am. Chem. Soc.* **2007**, *129*, 3458. doi:10.1021/JA0668973

- [5] Y. Yamada, Y. Tomiyama, A. Morita, M. Ikekita, S. Aoki, *Chem-BioChem* **2008**, *9*, 853. doi:10.1002/CBIC.200700718
- [6] J. Yeow, A. Kaur, M. D. Ancomb, E. J. New, *Chem. Commun.* **2014**, 8181. doi:10.1039/C4CC03464C
- [7] P. Yan, M. W. Holman, P. Robustelli, A. Chowdhury, F. I. Ishak, D. M. Adams, *J. Phys. Chem. B* **2005**, *109*, 130. doi:10.1021/JP045793G
- [8] M. Harris, J. L. Kolanowski, E. S. O'Neill, C. Henoumont, S. Laurent, T. N. Parac-Vogt, E. J. New, *Chem. Commun.* **2018**, 12986. doi:10.1039/C8CC07092J
- [9] K. Leslie, D. Jacquemin, E. New, K. Jolliffe, *Chem. – Eur. J.* **2018**, *24*, 5569. doi:10.1002/CHEM.201705546
- [10] D. H. Williamson, P. Lund, H. A. Krebs, *Biochem. J.* **1967**, *103*, 514. doi:10.1042/BJ1030514
- [11] S.-J. Lin, L. Guarente, *Curr. Opin. Cell Biol.* **2003**, *15*, 241. doi:10.1016/S0955-0674(03)00006-1
- [12] W.-C. Cheng, M. J. Kurth, *Org. Prep. Proced. Int.* **2002**, *34*, 585. doi:10.1080/00304940209355784
- [13] J. X. Qiao, in *Heterocyclic Chemistry in Drug Discovery* (Ed. J. J. Li) **2013**, Ch. 10, pp. 398–470 (Wiley: Hoboken, NJ).
- [14] H. Pal, S. Nad, M. Kumbhakar, *J. Chem. Phys.* **2003**, *119*, 443. doi:10.1063/1.1578057
- [15] S. Nad, H. Pal, *J. Phys. Chem. A* **2001**, *105*, 1097. doi:10.1021/JP003157M
- [16] S. Saha, A. Samanta, *J. Phys. Chem. A* **2002**, *106*, 4763. doi:10.1021/JP013287A
- [17] E. J. New, *ACS Sens.* **2016**, *1*, 328. doi:10.1021/ACSSENSORS.6B00148
- [18] K. Yang, K. G. Leslie, S. Y. Kim, B. Kalionis, W. Chrzanowski, K. A. Jolliffe, E. J. New, *Org. Biomol. Chem.* **2018**, *16*, 619. doi:10.1039/C7OB03164E